THE JOURNAL OF BIOLOGICAL CHEMISTRY VOL. 288, NO. 43, pp. 31069–31079, October 25, 2013

Endoplasmic Reticulum Protein Quality Control Is Determined by Cooperative Interactions between Hsp/c70 Protein and the CHIP E3 Ligase*

Received for publication, April 21, 2013, and in revised form, August 16, 2013 Published, JBC Papers in Press, August 29, 2013, DOI 10.1074/jbc.M113.479345

Yoshihiro Matsumura[‡§], **Juro Sakai**[§], **and William R. Skach**[‡1]

From the [‡]*Department of Biochemistry and Molecular Biology, Oregon Health and Science University, Portland, Oregon 97239 and the* [§]*Division of Metabolic Medicine, Research Center for Advanced Science and Technology, The University of Tokyo, 4-6-1 Komaba, Meguro-ku, Tokyo 153-8904, Japan*

Background: The CHIP E3 ligase regulates Hsp70 pro-degradation activities.
Results: The P269A CHIP U-box mutation induces CHIP oligomerization and modulates nucleotide- and substrate-dependent interactions between the TPR domain and Hsp70 C terminus.
Conclusion: The U-box domain plays a key role in CHIP recruitment to Hsp70-client complexes, possibly by controlling oligomerization.
Significance: Hsp70-CHIP substrate triage is governed by complex allosteric interactions between multiple domains in both proteins.

The C terminus of Hsp70 interacting protein (CHIP) E3 ligase functions as a key regulator of protein quality control by binding the C-terminal (M/I)EEVD peptide motif of Hsp/c70(90) with its N-terminal tetratricopeptide repeat (TPR) domain and facilitating polyubiquitination of misfolded client proteins via its C-terminal catalytic U-box. Using CFTR as a model client, we recently showed that the duration of the Hsc70-client binding cycle is a primary determinant of stability. However, molecular features that control CHIP recruitment to Hsp/c70, and hence the fate of the Hsp/c70 client, remain unknown. To understand how CHIP recognizes Hsp/c70, we utilized a dominant negative mutant in which loss of a conserved proline in the U-box domain (P269A) eliminates E3 ligase activity. In a cell-free reconstituted ER-associated degradation system, P269A CHIP inhibited Hsc70-dependent CFTR ubiquitination and degradation in a dose-dependent manner. Optimal inhibition required both the TPR and the U-box, indicating cooperativity between the two domains. Neither the wild type nor the P269A mutant changed the extent of Hsc70 association with CFTR nor the dissociation rate of the Hsc70-CFTR complex. However, the U-box mutation stimulated CHIP binding to Hsc70 while promoting CHIP oligomerization. CHIP binding to Hsc70 binding was also stimulated by the presence of an Hsc70 client with a preference for the ADP-bound state. Thus, the Hsp/c70 (M/I)EEVD motif is not a simple anchor for the TPR domain. Rather CHIP recruitment involves reciprocal allosteric interactions between its TPR and U-box domains and the substrate-binding and C-terminal domains of Hsp/c70.

In eukaryotic cells, protein synthesis, folding, and assembly are subject to a stringent quality control system charged with the role of degrading proteins that fail to achieve a native conformation (1–7). Such a system requires a selective mechanism to discriminate misfolded from properly folded substrates, tag those substrates that are misfolded, and deliver them to cellular degradation machinery. Substrate recognition is mediated, in part, by a network of cellular chaperones that includes the Hsp40, Hsp70, and Hsp90 heat shock protein families. In addition to facilitating folding, these chaperones recruit ubiquitin ligases (E3) and conjugating enzymes (E2) that covalently attach polyubiquitin chains and ultimately target the substrate for degradation by the 26 S proteasome (8–10). Thus, the Hsp40-Hsp/c70 network directly facilitates both productive folding as well as substrate degradation. Although the precise mechanisms that control these opposing roles remain poorly understood, the ultimate fate of client proteins involves selective and temporal recruitment of accessory co-chaperones that regulate the Hsp/c70 binding cycle (5, 11–15).

The C terminus of Hsp70 interacting protein (CHIP)[2] is a key component in Hsp/c70-mediated protein triage (16–18). CHIP contains three distinct domains: i) an N-terminal tetratricopeptide repeat (TPR) domain that binds the EEVD motif on the C terminus of Hsp/c70, ii) a linker region involved in homodimerization, and iii) a C-terminal U-box domain with E3 ligase activity (16, 17, 19, 20). As such, CHIP provides a direct bridge between the Hsp40/Hsp/c70 chaperone network and the ubiquitin proteasome system (18). In combination with the E2 enzymes, UbcH5 and Ubc13 (21–24), CHIP is responsible for ubiquitinating proteins implicated in a

* This work was supported, in whole or in part, by National Institutes of Health Grants DK51818 and GM53457 (to W. R. S.). This work was also supported by grants from the American Cystic Fibrosis Foundation (to W. R. S.), the Manpei Suzuki Diabetes Foundation (to Y. M.), grants-in-aid for young scientists (to Y. M.), for scientific research (to J. S.), and for scientific research on innovative areas (to J. S.), and a grant from the Translational Systems Biology and Medicine Initiative (TSBMI) from the Ministry of Education, Science, Sports and Culture (MEXT), Japan.

[1] To whom correspondence should be addressed: Dept. of Biochemistry and Molecular Biology, Oregon Health and Science University, MC L-224, 3181 S. W. Sam Jackson Park Rd., Portland, OR 97231. Tel.: 503-494-7322; Fax: 503-494-8393; E-mail: skachw@ohsu.edu.

[2] The abbreviations used are: CBag, C-terminal domain of Bag-1; CFTR, cystic fibrosis transmembrane conductance regulator; CHIP, C-terminal Hsc70-interacting protein; ER, endoplasmic reticulum, ERAD; endoplasmic reticulum-associated degradation; RRL, rabbit reticulocyte lysate; TPR, tetratricopeptide repeat; Bis-Tris, 2-(bis(2-hydroxyethyl)amino)-2-(hydroxymethyl)propane-1,3-diol; TCA sol, TCA-soluble; Ni-NTA, nickel-nitrilotriacetic acid; Tricine, *N*-[2-hydroxy-1,1-bis(hydroxymethyl)ethyl]-glycine; CBB, Coomassie Brilliant Blue.

variety of diseases that include cystic fibrosis, neurodegeneration, and cancer (17, 25, 26).

Despite their importance in protein triage, molecular interactions between CHIP and Hsp/c70 that regulate client binding, release, and ubiquitination remain poorly understood (16, 22, 27–30). CHIP was originally reported to decrease Hsp70-substrate binding and Hsp70-mediated substrate refolding, as well as Hsp40 (Hdj-1 and Hdj-2)-stimulated ATPase activity (17, 19). In contrast, CHIP overexpression in heat-stressed cells was subsequently shown to increase Hsp/c70-dependent protein refolding (31) and Hsp/c70-substrate binding (32). Thus, under different circumstances, CHIP appears to stabilize Hsp/c70-client complexes to either promote a productive folding outcome or recruit E2 ubiquitin-conjugating enzymes. More recently, when examined *in vitro* using purified proteins, CHIP did not change ADP dissociation from Hsp70, ATP binding to Hsp70, or the half-life of Hsp70-client complex (33). The latter findings suggested that CHIP acts in a relatively passive manner by stochastically ubiquitinating substrates as they cycle on and off Hsp/c70 during attempted folding. Consistent with this interpretation, we previously showed that CHIP-mediated ubiquitination was primarily dependent on the duration of Hsp/c70-client binding cycle and its regulation by nucleotide exchange factors such as Bag1 (15). Thus, multiple mechanisms appear to control formation and outcome of the ternary CHIP-Hsp/c70-client complex. Understanding how components of this complex are recruited and thereby control client fate remains a major challenge.

The cystic fibrosis transmembrane conductance regulator (CFTR) is a well studied substrate for ER quality control (34–38). CFTR is a member of the ATP-binding cassette (ABC) transporter superfamily (ABCC7) and functions as a protein kinase A-regulated and ATP-dependent chloride channel at the apical membrane of epithelial cells. In most cell types, CFTR folding is intrinsically inefficient. Approximately 70% of wild-type CFTR and more than 99% of disease-related trafficking mutants (the most common being ΔF508) are ubiquitinated, exported to the cytosol, and degraded by the UPS via ER-associated degradation (2, 5, 7, 34, 38). CHIP is among several E3 ligases including RMA1, Nedd4-2, and gp78 that facilitate ubiquitination of misfolded CFTR molecules (17, 22, 39–41).

To better understand how CHIP facilitates degradation, we examined a dominant negative mutant (P269A), which lacks a conserved proline in the U-box domain that is required for E3 ligase activity (22, 32, 42). Our approach was to use an *in vitro* translation and degradation system that recapitulates ER-associated degradation in a native-like cellular environment. Importantly, this system is readily amenable to biochemical manipulation and lacks compensatory transcriptional and translational mechanisms. It is thus possible to perturb chaperone levels and activities without secondary consequences that typically complicate similar maneuvers in intact cells (43–46). Moreover, because CFTR is the only radiolabeled client protein, it is relatively simple to characterize CHIP, Hsp/c70, and CFTR interactions that are responsible for ubiquitination and degradation. Our results show that CHIP binding to Hsp/c70 is influenced by allosteric interactions between the i) TPR and U-box domains of CHIP and ii) nucleotide/client-binding and C-terminal domains of Hsp/c70. These results indicate that CHIP-mediated triage of Hsp/c70 clients involves a complex interplay between multiple domains that govern affinity of the TPR for the EEVD motif.

EXPERIMENTAL PROCEDURES

Plasmids

Bacteria expression plasmids pET-P269A-CHIP, pET-CHIP-TPR (amino acids 1–197), pET-CHIP-U-box (amino acids 197–303), and pET-CHIP-P269A-Ubox were generated from wild-type (WT) pET30-CHIP (provided by D. M. Cyr (22)) by PCR amplification and ligation into NcoI and XhoI sites of the pET30 plasmid (22). A BamHI and XhoI fragment of CBag (47, 48) was generated by PCR and ligated into the same sites of pGEX4T.1 to obtain pGEX4T.1-CBag. All PCR-amplified sequences were confirmed by DNA sequencing. Other plasmids used were described previously (15).

His and GST Tag Protein Expression and Purification

Recombinant proteins were expressed in *Escherichia coli* BL21(DE3) transformed with corresponding pET30 and pGEX4T.1 plasmids by induction with 0.3 mM isopropyl β-D-1-thiogalactopyranoside (at A_{600} = 0.6) and incubation for 6 h at 24 °C as described (15). Recombinant proteins were purified by TALON metal affinity or glutathione-uniflow resin (BD Biosciences) according to manufacturer's instructions, concentrated using 10- or 30-kDa cutoff Centricon filters (Millipore, Billerica, MA) with buffer replacement (protein storage buffer; 50 mM HEPES-NaOH, pH 7.5, 100 mM NaCl, and 1 mM DTT), flash-frozen, and stored at −80 °C. UbcH5a and Hdj-2 (49) were stored in the presence of 300 and 500 mM NaCl, respectively. Proteins were at least 90–95% pure as confirmed by SDS-PAGE and Coomassie Brilliant Blue (CBB) staining (see Fig. 1*A*). ATPase activity of purified His-Hsc70 was 0.36 min^{-1} in the absence of Hdj-2 and 0.96 min^{-1} in the presence of both Hdj-2 and CBag, in good agreement with previous studies (15, 48).

In Vitro Transcription and Translation

CFTR RNA was transcribed from pSP-CFTR plasmid (15, 37, 50) at 40 °C for 2 h as described previously (15), precipitated by LiCl, rinsed three times with 70% ethanol, and dissolved into double-distilled H_2O. CFTR *in vitro* translation was performed at 24 °C for 2 h in a reaction containing 50 ng/μl CFTR RNA, 40% (v/v) nuclease-treated rabbit reticulocyte lysate (RRL), and canine pancreas microsomes (3 to 4 A_{280}) precisely as described (15). Following translation, microsomes were pelleted at 180,000 × *g* for 10 min through 0.5 M sucrose in buffer A (50 mM HEPES-NaOH, pH 7.5, 100 mM KCl, 5 mM $MgCl_2$, and 1 mM DTT). The membrane pellet was rinsed once with 0.1 M sucrose in buffer A and resuspended in the same buffer at half-volume of original translation reaction.

In Vitro CFTR Degradation

Microsomal membranes containing newly synthesized radiolabeled CFTR were added to RRL lacking endogenous hemin (60–70% v/v, prepared precisely as described (15, 44, 50)) and incu-

bated at 37 °C. Recombinant proteins were added at the concentration indicated. At the times indicated, aliquots were precipitated in 20% trichloroacetic acid (TCA) and centrifuged at 16,000 × *g* for 10 min, and [^{35}S]methionine in the supernatant (TCA sol) was counted in a Beckmann LS6500 scintillation counter (15). Total ^{35}S in each sample was determined by counting an aliquot of the degradation reaction. Mock reactions were used to correct for nonspecific association of ^{35}S and translation of endogenous mRNA remnants. The percentage of protein degraded into TCA-soluble peptide fragments at each time point was determined by

$$\%\ \text{TCA soluble} = (\text{CFTR}(T_n - T_0) - \text{Mock}(T_n - T_0))/(\text{CFTR}(\text{total} - T_0) - \text{Mock}(\text{total} - T_o))\ 100 \quad \text{(Eq. 1)}$$

where T_n and T_0 are TCA-soluble counts at $T = n$ and $T = 0$ min, respectively.

The percentage of degradation restored by the addition of recombinant Hsc70, WT CHIP, and/or UbcH5a was determined at $T = 60$ min using the following formula

$$\%\ \text{restoration} = [(\%\ \text{TCA sol}_{\text{restore}} - \%\ \text{TCA sol}_{\text{P269A}})/(\%\ \text{TCA sol} - \%\ \text{TCA sol}_{\text{P269A}})]\ 100 \quad \text{(Eq. 2)}$$

where % TCA sol is the control reaction without P269A CHIP, % TCA $\text{sol}_{\text{P269A}}$ is the reaction with P269A CHIP, and %TCA $\text{sol}_{\text{restore}}$ is the reaction with P269A CHIP and Hsc70, WT CHIP, and/or UbcH5a. Values represent mean ± S.E. of three or more experiments.

IC_{50} of CFTR Conversion into Peptides for P269A CHIP and TPR Domain

Apparent IC_{50} values of CFTR conversion into peptides for P269A CHIP and TPR domain were obtained from a graphical fit of the data using the equation $I = C/(IC_{50} + C)$ where C is the concentration of CHIP (μM) and I is the inhibition fraction. $I = 1 - (\%\ \text{TCA sol}_{\text{CHIP}}/\%\ \text{TCA sol})$ where % TCA sol is obtained from the control reaction without CHIP and % TCA sol_{CHIP} is obtained from the parallel reaction containing P269A CHIP or CHIP (15).

Ubiquitination Assay and Immunoprecipitation

Degradation reactions (10 μl) were diluted into 250 μl of buffer B (20 mM HEPES-NaOH, pH 7.5, 150 mM NaCl, 1 mM EDTA, 1% Triton X-100, 0.1% SDS, 0.5% sodium deoxycholate) containing protease inhibitor mixture (Roche Applied Science) as described (15). For co-immunoprecipitation of Hsc70-CFTR complex, translation reaction or microsomes containing newly synthesized radiolabeled CFTR were diluted into 500 μl of buffer C (20 mM HEPES-NaOH, pH 7.5, 150 mM NaCl, 1 mM EDTA, 1% Triton X-100) containing protease inhibitor. For CFTR release from Hsc70, microsomes were incubated with 10 μM WT CHIP, P269A CHIP, or CBag in buffer A containing 0.1 M sucrose and 1 mM ATP at 24 °C. After incubation, 500 μl of ice-cold buffer C containing 10 mM EDTA was added, and lysate was clarified at 16,000 × *g* at 4 °C for 20 min. Mouse anti-(mono-/poly-)ubiquitin antibody (FK2, Biomol International, Plymouth Meeting, PA) or rabbit anti-Hsp/c70 antisera (gift of Dr. William J. Welch, 51) was added. Samples were rotated for 1 h at 4 °C, and 5 μl of ImmunoPure-immobilized Protein G (Pierce Biotechnology) or Affi-Gel protein A (Bio-Rad Laboratories) was added and rotated overnight. Samples were washed five times with buffer B or C and three times with Tris-buffered saline (TBS; 20 mM Tris-HCl, pH 7.5, and 137 mM NaCl) and eluted with SDS sample buffer. Eluates were separated on an SDS-PAGE gel and analyzed by phosphorimaging as described (15).

Immunoblotting

Immunoblotting was performed as described (15, 52). Briefly, proteins were transferred to a PVDF membrane (Bio-Rad Laboratories) after SDS-PAGE and blocked with 5% (w/v) skim milk in TTBS (20 mM Tris-HCl, pH 7.5, 137 mM NaCl, and 0.1% Tween 20) for 1 h prior to incubation with mouse anti-Hsp/c70 antibody (N-27, gift of Dr. W. J. Welch (51)), 1:5,000 or rabbit anti-CHIP (PC-711, EMD Chemicals, Gibbstown, NJ), 1:5,000. Membrane was washed five times with TTBS and incubated for 1 h with goat anti-mouse IgG-HRP (Bio-Rad Laboratories), 1:5,000 or goat anti-rabbit IgG-HRP (Bio-Rad Laboratories), 1:10,000. Membranes were washed again with TTBS, and proteins were visualized with SuperSignal West Pico chemiluminescent substrate (Thermo Scientific) and Fuji Film (Light Labs, Dallas, TX).

His-CHIP Pulldown

His-CHIP or His-P269A CHIP (25 μg) was loaded onto 10 μl of Ni-NTA beads (Qiagen, Valencia, CA) in buffer D (20 mM HEPES-NaOH, pH 7.5, 150 mM NaCl, 0.1% Triton X-100). Samples were rotated at 4 °C for 1 h and washed four times with buffer D. Translation reaction or lysed microsomes (as above) were then added to the beads in buffer C (final volume 250 μl) and rotated at 4 °C for 2 h. Beads were washed and eluted as described above, and eluates were separated on an SDS-PAGE gel and analyzed by CBB staining (His-CHIP) or phosphorimaging (CFTR). For interaction of His-CHIP with RRL Hsc70, 50 μl of RRL or desalted RRL (using PD-10 desalting column, GE Healthcare Biosciences, pre-equilibrated in 10 mM HEPES-NaOH, pH7.5) was added to CHIP-containing beads in buffer D with 5 mM $MgCl_2$ (final volume 60 μl) and mixed in the presence or absence of 3 mM ATP or ADP at 4 °C for 4 h. Beads were washed six times with buffer D containing 20 mM imidazole and eluted with 500 mM imidazole in TBS. Eluates were separated on an SDS-PAGE gel and subjected to CBB staining (His-CHIP) or immunoblotting (Hsc70).

CHIP Binding to Client-bound Hsc70

Two nmol of biotinylated G17A peptide (GenScript, Piscataway, NJ), corresponding to residues Gly-545 to Ala-561 in human CFTR (53), was loaded on 10 μl of NeutrAvidin-agarose (Thermo Scientific) in TBS and rotated at 24 °C for 1 h. Beads were washed three times with TBS and incubated with 500 pmol of GST-Hsc70 in 50 μl of buffer E (20 mM HEPES-NaOH, pH 7.5, 150 mM NaCl, 5 mM $MgCl_2$, 1 mM ATP, 0.1% Triton X-100) at 24 °C for 10 min. ATP was depleted by the addition of hexokinase (20 units/ml) and 2-deoxyglucose (20 mM) to stabilize Hsc70 binding. Beads were then washed three times with

buffer D containing 10 mM EDTA prior to the addition of 12.5 pmol of His-CHIP or His-P269A CHIP (final volume 50 μl) and incubation at 4 °C for 1 h. Beads were washed five times with buffer D and three times with TBS, prior to elution, SDS-PAGE, and immunoblotting.

GST-Hsc70 Pulldown

GST or GST-Hsc70 (200 pmol) were loaded on 10 μl of glutathione-uniflow resin (BD Biosciences) in buffer E containing 1 mM ATP, rotated at 4 °C for 1 h, and washed four times wash with buffer E containing 1 mM ATP. His-CHIP or His-P269A CHIP (200 pmol) was added (final volume 50 μl), and beads, rotated at 4 °C for 1 h, were washed five times with buffer D and three times with TBS, eluted with SDS sample buffer, and analyzed by SDS-PAGE and immunoblotting.

Analysis of Protein Conformation

Glutaraldehyde Cross-linking—WT or P269A CHIP (2 μg) was incubated with 0.025% (v/v) glutaraldehyde in 10 μl of protein storage buffer for 10 min at 30 °C (20, 32). The cross-linking reaction was stopped by the addition of SDS sample buffer and analyzed by 10% SDS-PAGE followed by CBB staining.

Blue Native PAGE—WT or P269A CHIP (5 μg) was mixed with Blue-Native sample buffer (0.5% (w/v) CBB-G250, 10 mM Bis-Tris-HCl, pH 7.0, 50 mM aminocaproic acid, 1% (w/v) *n*-dodecyl β-D-maltoside, 5% (w/v) sucrose, final volume 20 μl) and applied on a NativePAGE Novex 4–16% Bis-Tris gel (Life Technologies). NativeMark unstained protein standard (Life Technologies) was used for molecular weight estimation. Electrophoresis was carried out at 4 °C at 150 V for 45 min (cathode buffer = 50 mM Tricine, 15 mM Bis-Tris-HCl, pH 7.0, and 0.02% CBB-G250; anode buffer = 50 mM Bis-Tris-HCl, pH 7.0) and then at 250 V for 45 min after reducing CBB-G250 dye concentration to 0.002% (9). After running, the gel was stained with CBB.

Limited Proteolysis—WT or P269A CHIP (4 μg) was incubated with the indicated concentration of proteinase K in 10 μl of protein storage buffer for 10 min on ice. Reaction was stopped by the addition of 2 mM PMSF and boiled with SDS sample buffer. Aliquots were analyzed by 12% SDS-PAGE and CBB staining.

RESULTS

P269A CHIP Inhibits Hsc70-dependent CFTR Ubiquitination and Degradation—To investigate the mechanism of CHIP-mediated client recognition, CFTR was expressed in a cell-free RRL translation/degradation system in the presence of ER microsomes and [^{35}S]methionine (15, 37, 50). In this system, CFTR is primarily generated as a full-length, ~160-kDa radiolabeled protein that is membrane-integrated and contains both nonglycosylated and core-glycosylated forms (37 and data not shown). Extensive studies in our laboratory have shown that CFTR ubiquitination is inefficient during translation at 24 °C, which allows us to temporally separate protein synthesis from subsequent degradation-related events (15, 37, 50, 54). However, when ER microsomes containing newly synthesized CFTR are isolated and incubated at 37 °C in RRL lacking exogenous hemin, CFTR is rapidly converted into a high molecular weight ubiquitinated species and subsequently degraded into TCA-soluble peptide fragments by the 26 S proteasome (15, 37) (Fig. 1, *B* and *C*). The addition of recombinant P269A CHIP (Fig. 1*A*) stabilized full-length CFTR (Fig. 1*B*, *lanes 5–12*) and inhibited CFTR cleavage in a dose-dependent manner (Fig. 1*D*). In contrast, the addition of WT CHIP had only a marginal effect in increasing CFTR degradation (1.25-fold) (Fig. 1, *C* and *E*), which likely reflects the robust degradation activity of RRL where CHIP is not a limiting. factor. The IC_{50} of P269A CHIP (2.5 μM) is similar to the Hsc70 concentration in RRL (2 μM) 15) (Fig. 1, *D* and *F*), although actual stoichiometry depends on protein oligomerization status (see Fig. 3).

CFTR immunoprecipitation using anti-ubiquitin antibody demonstrated that P269A CHIP also decreased substrate ubiquitination both in the presence and in the absence of the proteasome inhibitor MG132 (Fig. 1*G*). The inhibitory effect P269A CHIP was restored to 77% of control level by the readdition of purified recombinant Hsp70, WT CHIP, and UbcH5a proteins (Fig. 1, *H* and *I*; note that the Hsc70 is the dominant Hsp70 family member in RRL and is referred to as such in these experiments). Thus, consistent with cell-based studies, P269A CHIP acts in a dominant negative manner *in vitro* to inhibit Hsc70-dependent CFTR ubiquitination and degradation.

Both the U-box and the TPR Domain of P269A CHIP Are Required for Optimal inhibition of CFTR Degradation—We next used recombinant U-box and TPR domains from WT and P269A CHIP to determine which domain(s) were responsible for inhibiting degradation (17, 20, 22) (Fig. 2*A*). As expected, the isolated U-box domain from either WT or P269A CHIP failed to inhibit CFTR degradation (Fig. 2, *B* and *C*). In contrast, the addition of the TPR domain decreased CFTR degradation (Fig. 2*D*) as has been shown previously in intact cells (17). Surprisingly, however, the TPR construct was nearly 20-fold less potent than full-length P269A CHIP (apparent IC_{50} of 36 μM, Figs. 1*F* and 2*E*). Note that this effect is unlikely to be due to TPR degradation in RRL as the recombinant protein is present in ~1000-fold excess of our typical degradation substrates (*e.g.* CFTR). These results indicate that the TPR domain of P269A CHIP does not compete for Hsc70 binding in a simple manner with the TPR from WT CHIP. Rather, inhibition appears to involve a more complex interaction with the mutant U-box domain.

The P269A Mutation Alters CHIP Conformation and Stimulates Oligomerization—How might P269A exert its effect on other CHIP domains? Several studies have shown the functional importance of CHIP oligomerization. CHIP is natively dimeric, and dimerization of CHIP is essential for the E3 ubiquitin ligase activity (20). Heat treatment induces CHIP oligomerization and promotes chaperone function (32). We therefore investigated the oligomeric state of WT and P269A CHIP by chemical cross-linking (20, 32) and Blue Native-PAGE. Prior to cross-linking, both proteins migrated as ~40-kDa monomers on SDS-PAGE (Fig. 3*A*). After cross-linking, WT CHIP migrated primarily as an ~80-kDa dimer with some larger oligomeric forms (>250 kDa) as reported (20, 32). P269A CHIP was also oligomeric but yielded slightly less cross-linked dimer than WT (Fig. 3*A*, *lane 4*). Blue Native-PAGE (in the absence of cross-linker) further indicated that both proteins are oligo-

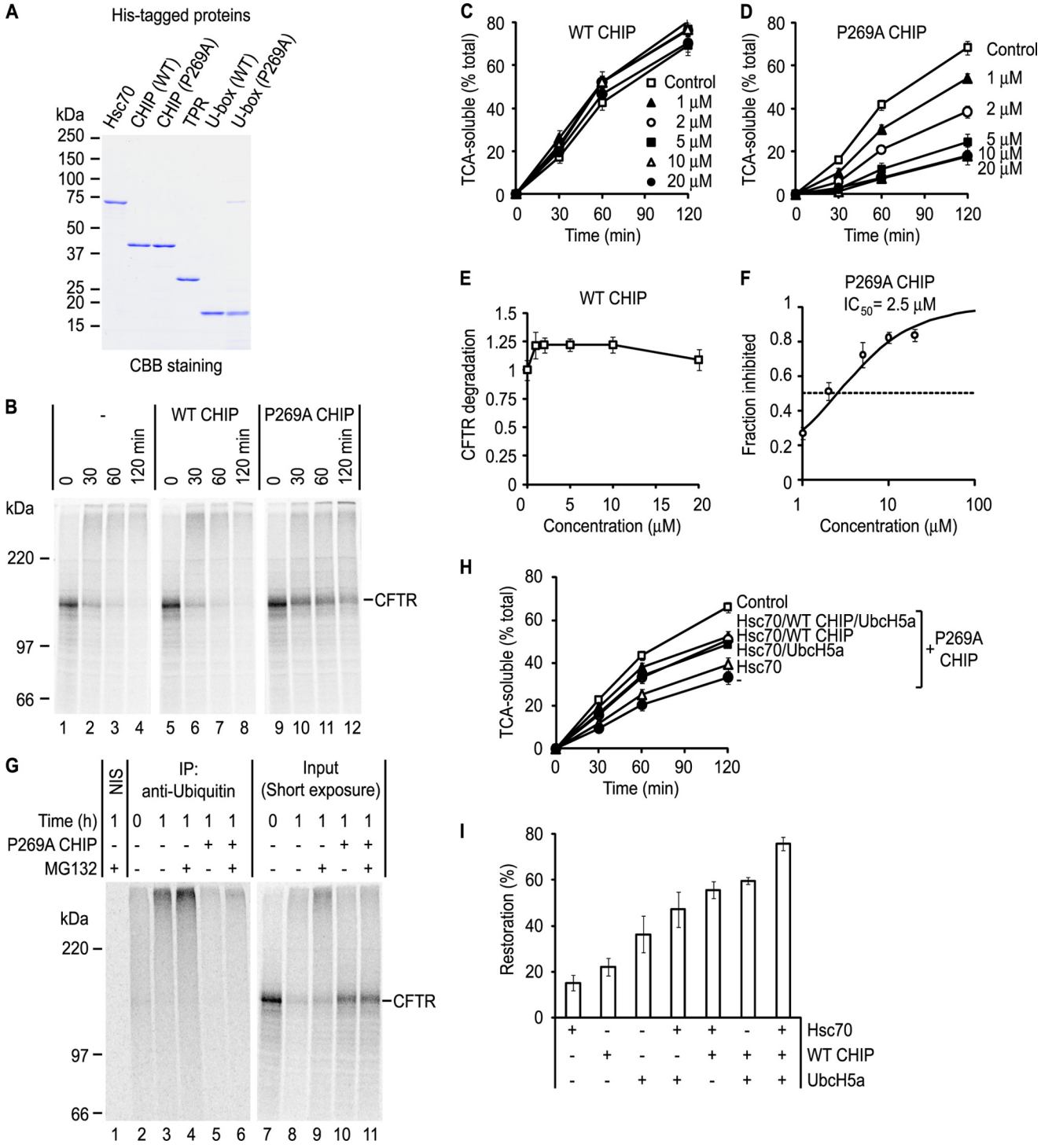

FIGURE 1. **P269A CHIP inhibits CFTR ubiquitination and degradation *in vitro*.** *A*, recombinant His-tagged proteins. Each His-tagged protein was purified, and 1 μg was separated on SDS-PAGE and stained with CBB. *B*, CFTR was translated in RRL in the presence of canine pancreas rough microsomes and [^{35}S]Met. Pelleted microsomes were incubated in an *in vitro* degradation reaction in the absence (*left*) or presence of 10 μM WT (*middle*) or P269A CHIP (*right*). Aliquots were analyzed by SDS-PAGE and phosphorimaging at the indicated times. *C* and *D*, CFTR conversion to TCA-soluble fragments in the presence and absence of WT CHIP (*C*) or P269A CHIP (*D*) (mean ± S.E. $n = 3–4$). *E*, CFTR conversion into TCA-soluble fragments at 60 min in the presence of the indicated concentration of WT CHIP normalized to control reaction without CHIP. *F*, apparent IC_{50} values of P269A CHIP. Data show the fraction of CFTR converted into TCA-soluble peptides that was inhibited by the addition of P269A CHIP as determined under "Experimental Procedures." *G*, phosporimage of *in vitro* synthesized CFTR subjected to *in vitro* degradation for 1 h in the presence of 10 μM P269A CHIP and/or 100 μM MG132. Samples were immunoprecipitated (*IP*) with anti-ubiquitin antibody (FK2) or nonimmune sera (*NIS*) prior to SDS-PAGE. *Right gel* shows 20% input for immunoprecipitation. *H*, CFTR degradation in the absence (*Control*) or presence of 3 μM P269A CHIP and combination of 10 μM Hsc70, WT CHIP, and/or UbcH5a as indicated. Graph shows the percentage of CFTR converted to TCA-soluble fragments at each point (mean ± S.E., $n = 3–5$). *I*, quantification of data as in *panel H* showing the extent of degradation inhibition by P269A CHIP that was restored by the addition of recombinant protein (mean ± S.E. $n = 3–5$).

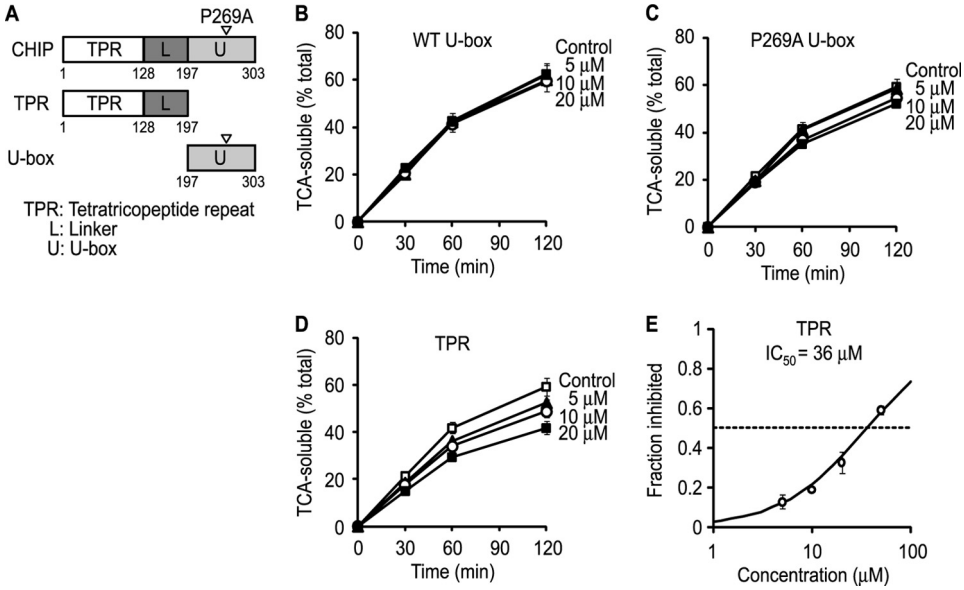

FIGURE 2. **U-box and TPR domains are both required for optimal inhibition of CFTR degradation.** *A*, diagram of CHIP, U-box, and TPR constructs showing the location of P269A mutation. *B–D*, CFTR degradation (as in Fig. 1) in the absence (*Control*) and presence of recombinant WT U-box (*B*), P269A U-box proteins (*C*), or TPR (*D*) (mean ± S.E. $n = 3$). *E*, apparent IC_{50} Values of TPR. Data show the fraction of CFTR converted into TCA-soluble peptides that was inhibited by the addition of TPR domain.

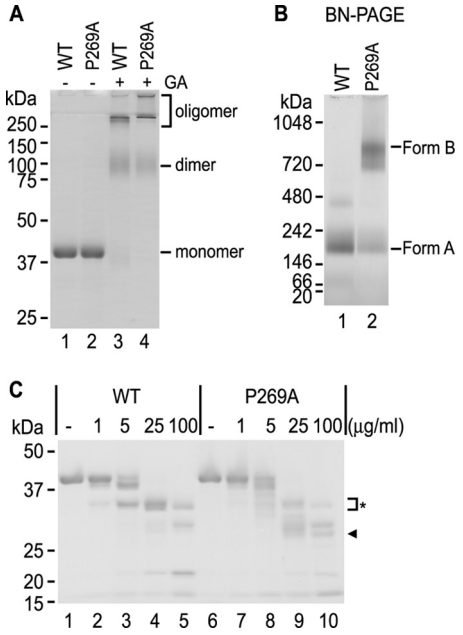

FIGURE 3. **P269A CHIP forms higher order oligomers than wild-type CHIP.** *A*, His-tagged WT or P269A CHIP (5 μM) was incubated with glutaraldehyde for 10 min at 30 °C. The cross-linking reaction was stopped by the addition of SDS sample buffer and analyzed by 12% SDS-PAGE followed by CBB staining. *B*, WT or P269A CHIP was analyzed by 4–16% Blue-Native PAGE followed by CBB staining. *C*, WT or P269A CHIP (10 μM) was incubated with the indicated concentration of proteinase K for 10 min on ice. Reaction was stopped by the addition of PMSF and boiled with SDS sample buffer. Aliquots were analyzed by 12% SDS-PAGE and CBB staining.

meric in solution, although P269A CHIP was predominantly found to reside in a larger complex (Form B) than WT CHIP (Form A) (Fig. 3*B*). Accounting for the theoretical molecular weight of CHIP dimer (80 kDa), it is likely that CHIP migrates aberrantly on Blue-Native PAGE, similar to its reported behavior during gel filtration (20), thereby making it difficult to determine the precise stoichiometry. However, P269A appears to stimulate formation of larger (and/or more stable) oligomers. Finally, P269A CHIP was more susceptible to limited proteinase K digestion as demonstrated by early cleavage of a major 35-kDa proteolytic fragment generated from WT protein (Fig. 3*C*). Thus, in addition to stimulating formation of large oligomeric complexes, P269A alters CHIP structure by inducing a more protease-accessible confirmation (open conformation).

P269A CHIP Does Not Affect CFTR Association with Hsc70 or Kinetics of Hsc70-CFTR Release—CHIP has been reported to affect Hsp/c70-client binding, Hsp/c70-mediated ATP hydrolysis, and client refolding (19, 32). We therefore tested whether the P269A mutation interfered with Hsc70 binding to CFTR by co-immunoprecipitation from RRL using anti-Hsp/c70 antisera. Results, shown in Fig. 4, *A* and *B*, demonstrate that the addition of either WT or P269A CHIP at levels that inhibit degradation (10 μM) had no detectable effect on the amount of CFTR bound to Hsc70 under basal conditions. In contrast, the addition of the C-terminal domain of Bag-1 (termed CBag (47, 55)), which stimulates Hsc70 ADP-ATP exchange, markedly reduced CFTR-Hsc70 binding as shown previously (15) (Fig. 4, *A* and *B*).

CHIP was originally shown to suppress Hsp40-stimulated Hsp70 ATPase activity and to stimulate client binding to Hsp70 (17, 19). These results suggested that CHIP might increase stability of the Hsc70-client complex by reducing turnover of the Hsp70 binding cycle. We therefore tested whether CHIP might alter the kinetics of CFTR release from Hsc70, which is triggered by ADP-ATP exchange. When ER microsomes containing Hsc70-CFTR complexes were isolated from RRL in the absence of ATP, CFTR remained stably bound to Hsc70. In contrast, ATP addition resulted in dissociation of Hsc70, which was further stimulated by the addition of CBag (Fig. 4, *C* and *D*) consistent with previous results (15). Importantly, the addition of WT or P269A CHIP (plus ATP) had no effect on either the amount of CFTR bound or the rate of Hsc70-CFTR dissociation

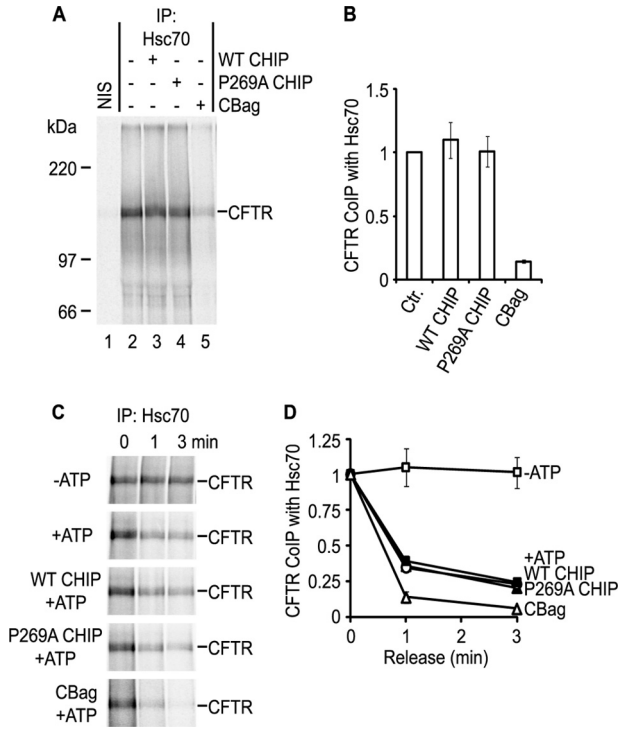

FIGURE 4. **CHIP does not affect Hsc70-CFTR binding or kinetics of dissociation.** *A*, following CFTR synthesis, WT CHIP, P269A CHIP, or CBag was added to the translation reaction, and microsomes were collected, solubilized, and immunoprecipitated (*IP*) with nonimmune sera (*NIS*) or anti-Hsc70 antisera prior to SDS-PAGE and phosphorimaging. *B*, quantification of CFTR-Hsc70 co-immunoprecipitation as shown in *panel A* (mean ± S.E. $n = 3–4$). *C*, microsomes containing newly synthesized CFTR were solubilized in Triton X-100 and immunoprecipitated with anti-Hsc70 antisera 0, 1, or 3 min after the addition of ATP, WT CHIP, P269A CHIP, or CBag as indicated. *D*, quantification of co-immunoprecipitation as shown in *panel C* (mean ± S.E. $n = 3–4$).

above that observed for ATP alone (Fig. 4, *C* and *D*). Similarly, the steady state ATPase activity of Hsc70 (in the presence or absence of Hdj-2) was also not affected by the addition of equimolar WT or P269A mutant CHIP (data not shown). These results indicate that P269A CHIP inhibits CFTR degradation by a mechanism other than altering stability of Hsc70-CFTR interactions or duration of Hsc70-CFTR binding cycle.

P269A CHIP Recognizes CFTR-Hsc70 Complex More Efficiently than WT CHIP—Because TPR and U-box domains are both required to optimally inhibit CFTR degradation, we next tested whether the P269A mutation might allosterically alter affinity of the TPR for the Hsc70-CFTR complex. Microsomes containing newly synthesized, radiolabeled CFTR were isolated from RRL either after ATP depletion (to stabilize Hsc70 binding) or after incubation with ATP and CBag (to release Hsc70 from CFTR, Fig. 5*A*, *lanes 2* and *4*, respectively). Following solubilization, samples were then incubated with excess His-tagged WT CHIP or P269A CHIP, and bound CFTR was isolated using nickel-NTA affinity resin. In the absence of ATP, approximately four times more CFTR was recovered with P269A CHIP than WT CHIP under identical conditions (Fig. 5*B*, *lanes 1–3*, and 5*C*). The addition of ATP and CBag released most CFTR from Hsc70, although a small amount of CFTR was still pulled down by P269A CHIP but not WT CHIP (Fig. 5*B*, *lanes 5* and *6*).

To confirm that CHIP does not bind CFTR directly, microsomes containing Hsc70-CFTR complexes were isolated and incubated for 3 min in either the absence of ATP or the presence of CBag plus ATP, and samples were affinity-purified with His-CHIP as described above (Fig. 5*D*). Again, severalfold more CFTR was recovered by P269A CHIP than WT CHIP in the

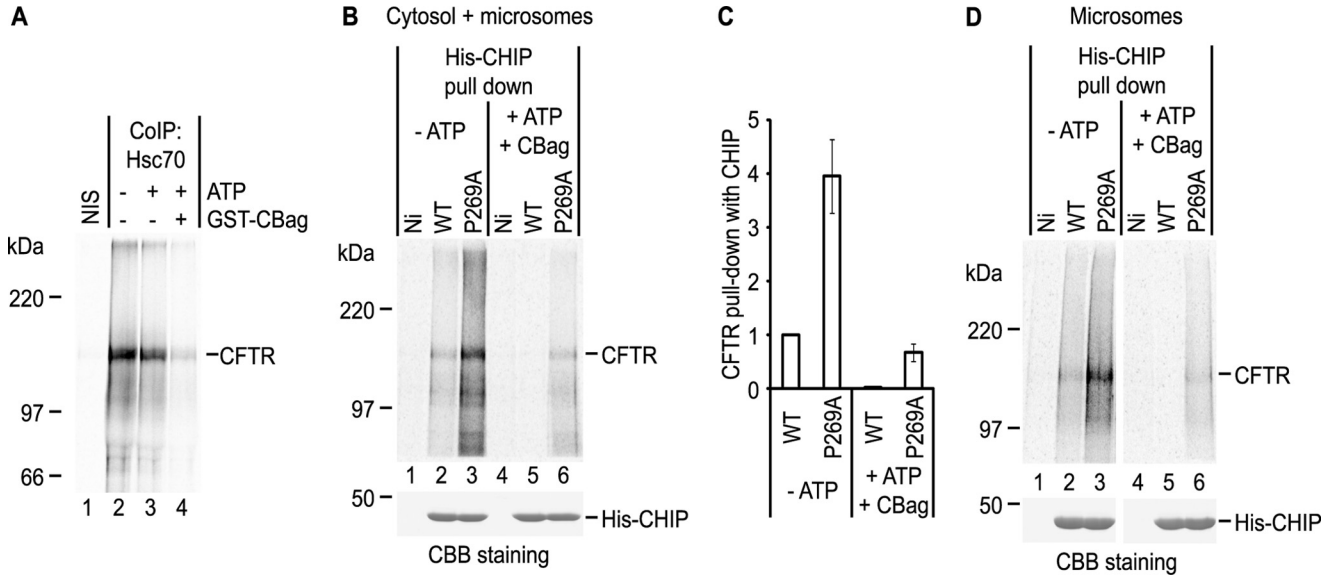

FIGURE 5. **P269A increases CHIP binding to Hsc70-CFTR complex.** *A*, CFTR was synthesized in RRL and treated with hexokinase/2-deoxy glucose (*−ATP*) or ATP and/or GST-CBag for 10 min. Microsomes were then isolated, solubilized, and immunoprecipitated (*IP*) with nonimmune sera (*NIS*) or anti-Hsc70 antisera. *B*, following synthesis, the translation reaction was incubated with hexokinase/2-deoxyglucose or GST-CBag plus ATP as in *panel A*. Microsomes were collected and solubilized, and CFTR was affinity-purified with immobilized His-tagged WT CHIP, P269A CHIP, or Ni-NTA (*Ni*, control). *C*, quantification of experiments as shown in *panel B* (mean ± S.E. $n = 3$). *D*, microsomes were isolated after ATP depletion as in *panel A* and further incubated for 3 min in buffer (without ATP) or in the presence of CBag plus ATP to remove bound Hsc70, prior to affinity pulldown with His-tagged WT or P269A CHIP.

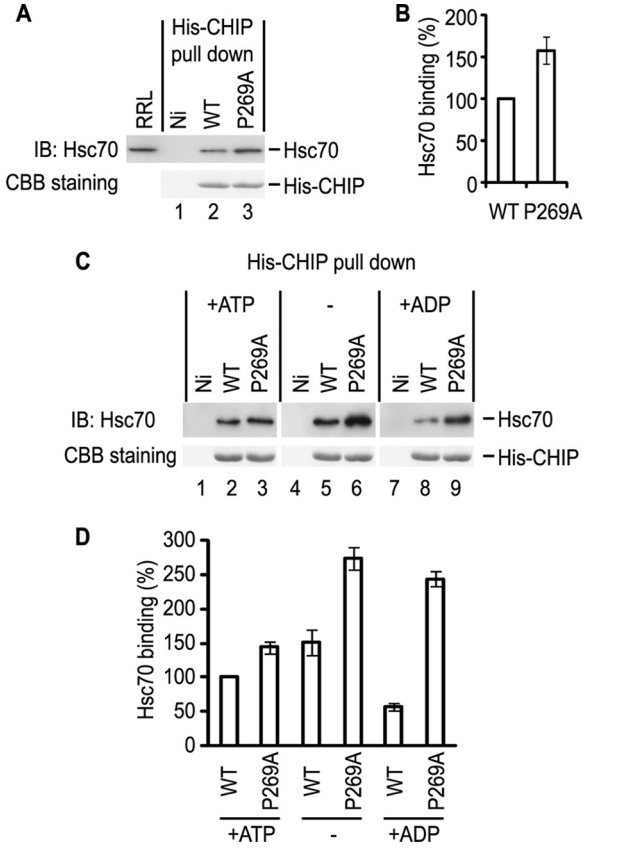

FIGURE 6. **P269A CHIP preferentially binds ADP-Hsc70.** *A*, Hsc70 was recovered from RRL using immobilized His-tagged WT or P269A CHIP, or Ni-NTA (*Ni*). *IB*, immunoblot. *B*, quantification of experiments as shown in *panel A* (mean ± S.E. $n = 4$). *C*, Hsc70 was affinity-isolated as in *panel A*, but using desalted RRL supplemented with ATP, ADP, or no nucleotide as indicated. Recovered Hsc70 was detected by immunoblotting. *D*, quantification of experiments as shown in *panel C* (mean ± S.E. $n = 4$).

ATP-depleted samples (Fig. 5*D*, *lanes 2* and *3*), whereas Hsc70 release prior to the addition of CHIP eliminated CFTR recovery by WT CHIP and markedly decreased CFTR pulldown for the P269A mutant (Fig. 5*D*, *lanes 5* and *6*). Thus, CHIP binding to CFTR occurs indirectly via ATP-sensitive interactions, likely with the Hsc70-CFTR complex. This interaction is strongly increased by the P269A U-box mutation.

The P269A Mutation Increases Hsc70 Binding in a Nucleotide-dependent Manner—Results of Fig. 5 suggest that the dominant negative phenotype exhibited by P269A CHIP is due at least in part to an increased affinity for Hsc70. We therefore immobilized recombinant WT and mutant His-CHIP as bait to pull down endogenous Hsc70 from RRL. Unexpectedly, P269A CHIP exhibited only a modest increase (1.5-fold) in Hsc70 binding as compared with WT CHIP (Fig. 6, *A* and *B*). However, RRL likely contains a mixture of client-bound and unbound Hsc70 in various states of nucleotide occupancy. RRL was therefore desalted by gel filtration to remove endogenous nucleotides and then supplemented with ATP (to promote client release), ADP, or no nucleotide to stabilize client binding. In the presence of excess ATP, P269A CHIP bound Hsc70 1.5-fold better than WT CHIP (Fig. 6*C*, *lanes 1–3*, and 6*D*). In the absence of nucleotide, there was an increase in base-line Hsc70 recovery for WT CHIP, and this effect was further accentuated for mutant CHIP (Fig. 5*C*, *lanes 4–6*, and 6*D*). Interestingly, the addition of ADP, which is expected to stabilize Hsc70-client complexes, resulted in nearly a 5-fold increase in Hsc70 binding to mutant over WT CHIP (Fig. 6*C*, *lanes 7–9*, and 6*D*). It is not clear why Hsc70 binding to WT CHIP was reduced in the presence of ADP, but this effect may reflect heterogeneity of client complexes or Hsc70 regulatory co-factors. Taken together, these results provide evidence that nucleotide occupancy of the N-terminal domain of Hsc70 allosterically influences the affinity of its C-terminal EEVD motif for CHIP, and this effect is more pronounced for U-box mutant, which strongly favors the ADP bound conformation.

Hsc70 Client Loading Stimulates P269A CHIP Binding—Given that Hsc70-client binding is stabilized by ADP, one possibility is that affinity of the CHIP TPR domain for Hsc70 is influenced by occupancy of the substrate-binding cleft. Because it is difficult to determine the fraction of Hsc70 that is bound to clients in cytosolic extracts, we tested this hypothesis using recombinant proteins and a known peptide substrate derived from NBD1 of CFTR (Gly-545 to Ala-561, G17A peptide) (53). Biotinylated G17A peptide was immobilized on NeutrAvidin-agarose, and beads were incubated with purified recombinant GST-Hsc70 protein (Fig. 7*A*). To facilitate client loading, binding was initiated in the presence of ATP for 10 min and then treated with hexokinase to convert remaining nucleotide to ADP (ATP depletion) or ATP-containing buffer (Fig. 7*B*). Hsc70 binding to beads was undetectable in the absence of peptide, whereas binding was readily observed following ATP depletion as expected (Fig. 7*B*). This observation allowed us to compare the interaction of WT and P269A CHIP specifically with client-bound Hsc70 (Fig. 7*C*). Neither form of CHIP bound to peptide in the absence of Hsc70. However, both forms were recovered from the Hsc70-client complex, with 3-fold more mutant CHIP recovered than WT CHIP (Fig. 7*C*), which is in good agreement with the increase in CFTR recovery by mutant CHIP (Fig. 5, *B* and *C*).

To further confirm that the U-box mutation selectively increases affinity of CHIP to the client-bound form of Hsc70, GST-Hsc70 was immobilized on glutathione resin in the presence of ATP to remove residual client proteins. Beads were then incubated with WT or P269A CHIP. Results reveal that in the absence of an Hsc70 client, P269A CHIP binding was only slightly increased (~1.5-fold) over WT CHIP (Fig. 7*D*), which is similar to the difference observed for CHIP binding to Hsc70 in RRL (Fig. 6, *C* and *D*).

DISCUSSION

In this study, we used a reconstituted cell-free system to better understand how CHIP-Hsp/c70-client complex formation contributes to quality control of a prototypical ER-associated degradation substrate. Our results demonstrate that dominant negative P269A CHIP, which lacks E3 ligase activity (22, 32, 42), strongly inhibits Hsc70-dependent CFTR ubiquitination and degradation. Interestingly, inhibition does not occur via a simple competition with the WT CHIP TPR domain (56, 57). Rather, the U-box mutation increases the efficiency of CHIP binding to Hsc70 (presumably to the C-terminal EEVD motif) over that of WT CHIP without affecting the rate of Hsc70-

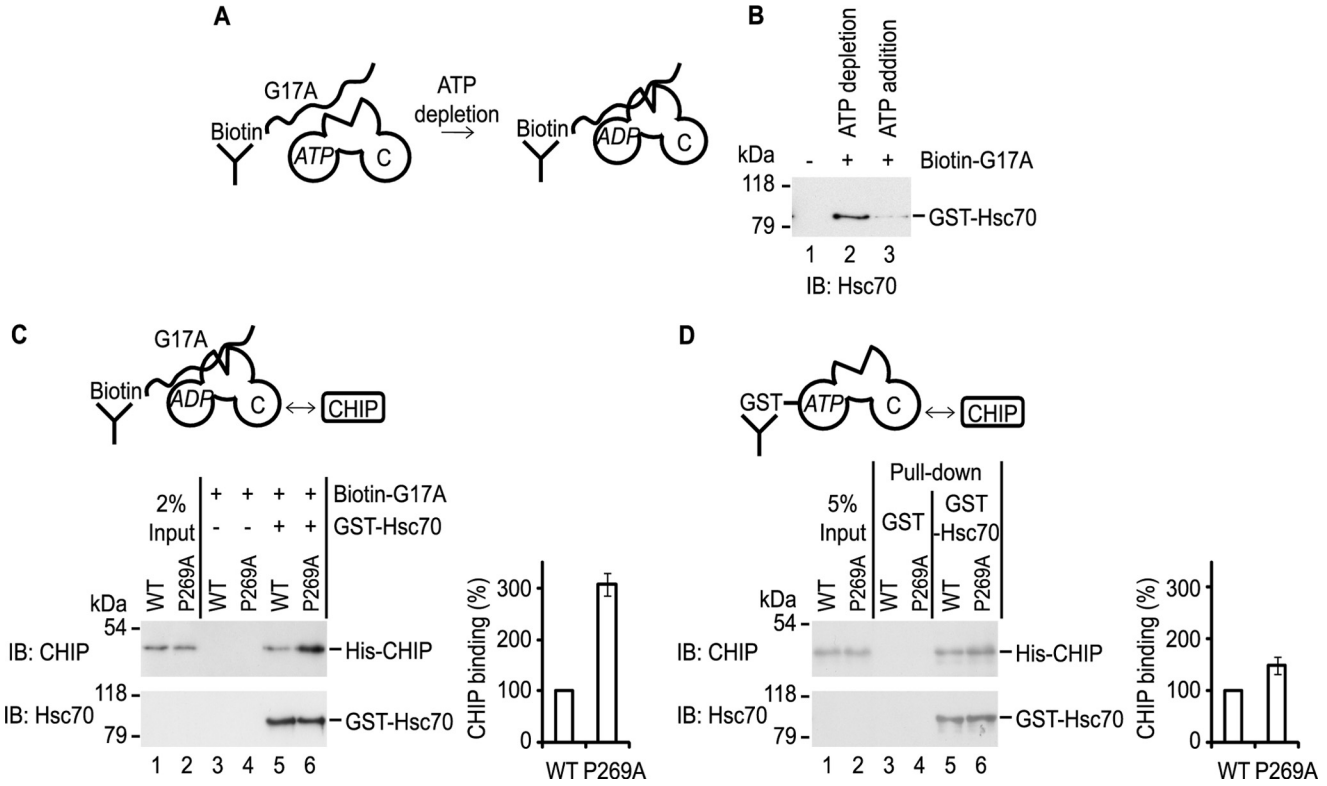

FIGURE 7. **P269A CHIP preferentially binds client-bound Hsc70.** *A*, schematic of strategy to isolate client-bound Hsc70. *B*, recombinant GST-Hsc70 was incubated with biotinylated G17A peptide immobilized on NeutrAvidin-agarose in the presence of ATP. After 10 min of incubation, ATP was depleted or sample was diluted with buffer containing ATP to release client. Bound GST-Hsc70 was eluted with SDS and immunoblotted (*IB*) with anti-Hsc70 antisera. *C*, *in vitro* binding assay between G17A-bound GST-Hsc70 and CHIP. His-tagged WT CHIP or P269A CHIP was incubated with immobilized G17A peptide-bound GST-Hsc70. After washing, His-CHIP and Hsc70 were eluted with SDS and analyzed by immunoblotting. *D*, binding assay between client-free GST-Hsc70 and WT or P269A CHIP. His-tagged WT or P269A CHIP was incubated with GST (control) or GST-Hsc70 immobilized on glutathione resin. After washing, His-CHIP was eluted with SDS and analyzed by immunoblotting. Parallel immunoblotting with anti-Hsc70 confirmed equal loading of GST-Hsc70. Graphs show mean ± S.E. ($n \geq 3$).

mediated ATP hydrolysis or the kinetics of ATP-mediated client release. This effect was also observed using recombinant components in the absence of ubiquitin and E2 enzymes. Thus, CHIP binding to Hsc70 is subject to allosteric interactions between the TPR and U-box domains independent of substrate ubiquitination. These functional findings raise the possibility that the U-box contributes to induced folding of the highly flexible TPR domain during binding to the EEVD peptide motif (57). Consistent with this notion, limited proteolysis revealed that P269A does not simply disrupt catalytic activity, but also induces structural changes that result in a more open (protease-sensitive) conformation. Surprisingly, this structural change was also associated with formation of large oligomers with increased affinity for Hsc70.

A second finding was that the preferential interaction of Hsc70 with P269A CHIP is dependent upon occupancy of the Hsc70 client-binding cleft. This was observed by manipulating both ADP and ATP availability in RRL, which mimics native cytosolic conditions, and with a defined peptide substrate using recombinant proteins. Given the dynamic nature of the Hsp/c70 binding cycle, our findings impose an additional layer of control on CHIP recruitment that depends not only on the interplay between TPR and U-box domains of CHIP, but also on cross-talk between the client-binding domain, the C terminus, and possibly the ATPase domain of Hsc70. Thus, formation and stability of CHIP-Hsc70-client complexes do not necessarily result from nonspecific binding, as has been suggested (58), but rather involve multiple domains in both proteins, and potentially CHIP oligomerization, which regulates TPR-EEVD affinity.

CHIP was originally identified as a co-chaperone and negative regulator of Hsp/c70 (19) and later shown to function as a U-box ubiquitin E3 ligase for a variety of Hsp/c70 client proteins (16, 17). For the majority of substrates, CHIP-mediated ubiquitination is obligatorily coupled to Hsp70 and thus is dependent on the Hsp/c70 binding cycle (22, 27–30). In this cycle, Hsp/c70 recruits clients in its ATP-bound state and then forms a stable complex upon ATP hydrolysis. Substrate release is stimulated by spontaneous or nucleotide exchange factor-mediated ATP/ADP exchange (5, 55). Although early studies suggested that CHIP suppresses Hsp40-stimulated Hsp/c70 ATPase activity and inhibits Hsp/c70-client binding (17, 19), our results show that for CFTR, it does not affect either Hsc70 association (Fig. 4, *A* and *B*) or duration of Hsc70-CFTR binding in a single release cycle (Fig. 4, *C* and *D*). These findings are consistent with recent studies from the Mayer group (33), which concluded that recruitment of CHIP to Hsp70-client complexes is a decisive factor in triaging pro-folding from pro-degradation outcomes. However, our results provide evidence that CHIP recruitment to Hsc70 is not solely a passive process, but one that can be actively modulated by client binding (shown here) in addition to posttranslational modification (*e.g.* phos-

phorylation) (59). Thus, it would follow logically that increased affinity for the Hsp70-client complex, over Hsc70 alone, would enable CHIP to more efficiently interact with the cellular pool of Hsp/c70 that is actively engaged with unfolded potential ubiquitination targets (33).

An important objective in protein folding diseases such as cystic fibrosis is to devise strategies in which misfolded, but potentially functional, proteins can be rescued from ER-associated degradation and delivered to their cellular site of function. Because of its central role in both folding and degradation, the Hsp40/70 network provides a potential target for such a manipulation (14). Indeed, evidence suggests that blocking Hsp/c70 function (60–63) or manipulating Hsp40 cochaperones (11, 12, 64, 65) can protect a subpopulation of newly synthesized CFTR from degradation. Consistent with this, we recently showed that the duration of Hsc70-client binding cycle is a major determinant of CFTR ubiquitination and degradation (15). It is difficult, however, to manipulate Hsp/c70 function in intact cells due to the high expression levels and compensatory effects on the proteostatic network. Moreover, although Hsp/c70 inhibition might decrease degradation, it would also likely have broad and potentially deleterious effects on the cellular folding environment. In this respect, selectively targeting the degradation arm of Hsp/c70 through CHIP could potentially accomplish this goal while leaving pro-folding activities intact. Such a strategy might be to selectively block CHIP interactions while preserving interactions with other co-chaperones that compete for the EEVD binding (*e.g.* Hop) and recruitment of the Hsp90 maturation complex (57, 66). Although CHIP and Hop bind the EEVD motif with similar affinity (57, 58), the finding that substrate and nucleotide may modulate this process raises the possibility that specific substrate properties might impact which co-chaperones are ultimately recruited, and hence, the fate of the ternary complex.

Acknowledgments—We thank Dr. Jason C. Young for CBag and Hsc70 plasmids, Dr. Douglas M. Cyr for CHIP plasmid, Dr. William J. Welch for anti-Hsp/c70 antibody/sera, Zhongying Yang for technical assistance, and other members of the Skach laboratory for helpful discussions.

REFERENCES

1. Kopito, R. R. (1997) ER quality control: the cytoplasmic connection. *Cell* **88,** 427–430
2. Meusser, B., Hirsch, C., Jarosch, E., and Sommer, T. (2005) ERAD: the long road to destruction. *Nat. Cell Biol.* **7,** 766–772
3. Denic, V., Quan, E. M., and Weissman, J. S. (2006) ERAD: the long road to destruction. A luminal surveillance complex that selects misfolded glycoproteins for ER-associated degradation. *Cell* **126,** 349–359
4. Carvalho, P., Goder, V., and Rapoport, T. A. (2006) Distinct ubiquitin-ligase complexes define convergent pathways for the degradation of ER proteins. *Cell* **126,** 361–373
5. Vembar, S. S., and Brodsky, J. L. (2008) One step at a time: endoplasmic reticulum-associated degradation. *Nat. Rev. Mol. Cell Biol.* **9,** 944–957
6. Cross, B. C., Sinning, I., Luirink, J., and High, S. (2009) Delivering proteins for export from the cytosol. *Nat. Rev. Mol. Cell Biol.* **10,** 255–264
7. Brodsky, J. L., and Skach, W. R. (2011) Protein folding and quality control in the endoplasmic reticulum: Recent lessons from yeast and mammalian cell systems. *Curr. Opin. Cell Biol.* **23,** 464–475
8. Pickart, C. M., and Cohen, R. E. (2004) Proteasomes and their kin: proteases in the machine age. *Nat. Rev. Mol. Cell Biol.* **5,** 177–187
9. Shibatani, T., Carlson, E. J., Larabee, F., McCormack, A. L., Früh, K., and Skach, W. R. (2006) Global organization and function of mammalian cytosolic proteasome pools: Implications for PA28 and 19S regulatory complexes. *Mol. Biol. Cell* **17,** 4962–4971
10. Hirsch, C., Gauss, R., Horn, S. C., Neuber, O., and Sommer, T. (2009) The ubiquitylation machinery of the endoplasmic reticulum. *Nature* **458,** 453–460
11. Alberti, S., Böhse, K., Arndt, V., Schmitz, A., and Höhfeld, J. (2004) The cochaperone HspBP1 inhibits the CHIP ubiquitin ligase and stimulates the maturation of the cystic fibrosis transmembrane conductance regulator. *Mol. Biol. Cell* **15,** 4003–4010
12. Arndt, V., Daniel, C., Nastainczyk, W., Alberti, S., and Höhfeld, J. (2005) BAG-2 acts as an inhibitor of the chaperone-associated ubiquitin ligase CHIP. *Mol. Biol. Cell* **16,** 5891–5900
13. Dai, Q., Qian, S. B., Li, H. H., McDonough, H., Borchers, C., Huang, D., Takayama, S., Younger, J. M., Ren, H. Y., Cyr, D. M., Patterson, C. (2005) Regulation of the cytoplasmic quality control protein degradation pathway by BAG2. *J. Biol. Chem.* **280,** 38673–38681
14. Kampinga, H. H., and Craig, E. A. (2010) The HSP70 chaperone machinery: J proteins as drivers of functional specificity. *Nat. Rev. Mol. Cell Biol.* **11,** 579–592
15. Matsumura, Y., David, L. L., and Skach, W. R. (2011) Role of Hsc70 binding cycle in CFTR folding and endoplasmic reticulum-associated degradation. *Mol. Biol. Cell* **22,** 2797–2809
16. Connell, P., Ballinger, C. A., Jiang, J., Wu, Y., Thompson, L. J., Höhfeld, J., and Patterson, C. (2001) The co-chaperone CHIP regulates protein triage decisions mediated by heat-shock proteins. *Nat. Cell Biol.* **3,** 93–96
17. Meacham, G. C., Patterson, C., Zhang, W., Younger, J. M., and Cyr, D. M. (2001) The Hsc70 co-chaperone CHIP targets immature CFTR for proteasomal degradation. *Nat. Cell Biol.* **3,** 100–105
18. McDonough, H., and Patterson, C. (2003) CHIP: a link between the chaperone and proteasome systems. *Cell Stress Chaperones* **8,** 303–308
19. Ballinger, C. A., Connell, P., Wu, Y., Hu, Z., Thompson, L. J., Yin, L. Y., and Patterson, C. (1999) Identification of CHIP, a novel tetratricopeptide repeat-containing protein that interacts with heat shock proteins and negatively regulates chaperone functions. *Mol. Cell. Biol.* **19,** 4535–4545
20. Nikolay, R., Wiederkehr, T., Rist, W., Kramer, G., Mayer, M. P., and Bukau, B. (2004) Dimerization of the human E3 ligase CHIP via a coiled-coil domain is essential for its activity. *J. Biol. Chem.* **279,** 2673–2678
21. Jiang, J., Ballinger, C. A., Wu, Y., Dai, Q., Cyr, D. M., Höhfeld, J., and Patterson, C. (2001) CHIP is a U-box-dependent E3 ubiquitin ligase: identification of Hsc70 as a target for ubiquitylation. *J. Biol. Chem.* **276,** 42938–42944
22. Younger, J. M., Ren, H. Y., Chen, L., Fan, C. Y., Fields, A., Patterson, C., and Cyr, D. M. (2004) A foldable CFTRΔF508 biogenic intermediate accumulates upon inhibition of the Hsc70-CHIP E3 ubiquitin ligase. *J. Cell Biol.* **167,** 1075–1085
23. Zhang, M., Windheim, M., Roe, S. M., Peggie, M., Cohen, P., Prodromou, C., and Pearl, L. H. (2005) Chaperoned ubiquitylation–crystal structures of the CHIP U box E3 ubiquitin ligase and a CHIP-Ubc13-Uev1a complex. *Mol. Cell* **20,** 525–538
24. Xu, Z., Kohli, E., Devlin, K. I., Bold, M., Nix, J. C., and Misra, S. (2008) Interactions between the quality control ubiquitin ligase CHIP and ubiquitin conjugating enzymes. *BMC Struct. Biol.* **8,** 26
25. Dickey, C. A., Patterson, C., Dickson, D., and Petrucelli, L. (2007) Brain CHIP: removing the culprits in neurodegenerative disease. *Trends Mol. Med.* **13,** 32–38
26. Carraway, K. L., 3rd. (2010) E3 ubiquitin ligases in ErbB receptor quantity control. *Semin. Cell Dev. Biol.* **21,** 936–943
27. Xu, W., Marcu, M., Yuan, X., Mimnaugh, E., Patterson, C., and Neckers, L. (2002) Chaperone-dependent E3 ubiquitin ligase CHIP mediates a degradative pathway for c-ErbB2/Neu. *Proc. Natl. Acad. Sci. U.S.A.* **99,** 12847–12852
28. Zhou, P., Fernandes, N., Dodge, I. L., Reddi, A. L., Rao, N., Safran, H., DiPetrillo, T. A., Wazer, D. E., Band, V., and Band, H. (2003) ErbB2 degradation mediated by the co-chaperone protein CHIP. *J. Biol. Chem.* **278,** 13829–13837

29. Shimura, H., Schwartz, D., Gygi, S. P., and Kosik, K. S. (2004) CHIP-Hsc70 complex ubiquitinates phosphorylated tau and enhances cell survival. *J. Biol. Chem.* **279,** 4869–4876
30. Urushitani, M., Kurisu, J., Tateno, M., Hatakeyama, S., Nakayama, K., Kato, S., and Takahashi, R. (2004) CHIP promotes proteasomal degradation of familial ALS-linked mutant SOD1 by ubiquitinating Hsp/Hsc70. *J. Neurochem.* **90,** 231–244
31. Kampinga, H. H., Kanon, B., Salomons, F. A., Kabakov, A. E., and Patterson, C. (2003) Overexpression of the cochaperone CHIP enhances Hsp70-dependent folding activity in mammalian cells. *Mol. Cell. Biol.* **23,** 4948–4958
32. Rosser, M. F., Washburn, E., Muchowski, P. J., Patterson, C., and Cyr, D. M. (2007) Chaperone functions of the E3 ubiquitin ligase CHIP. *J. Biol. Chem.* **282,** 22267–22277
33. Stankiewicz, M., Nikolay, R., Rybin, V., and Mayer, M. P. (2010) CHIP participates in protein triage decisions by preferentially ubiquitinating Hsp70-bound substrates. *FEBS J.* **277,** 3353–3367
34. Cheng, S. H., Gregory, R. J., Marshall, J., Paul, S., Souza, D. W., White, G. A., O'Riordan, C. R., and Smith, A. E. (1990) Defective intracellular transport and processing of CFTR is the molecular basis of most cystic fibrosis. *Cell* **63,** 827–834
35. Ward, C. L., and Kopito, R. R. (1994) Intracellular turnover of cystic fibrosis transmembrane conductance regulator. Inefficient processing and rapid degradation of wild-type and mutant proteins. *J. Biol. Chem.* **269,** 25710–25718
36. Ward, C. L., Omura, S., and Kopito, R. R. (1995) Degradation of CFTR by the ubiquitin-proteasome pathway. *Cell* **83,** 121–127
37. Xiong, X., Chong, E., and Skach, W. R. (1999) Evidence that endoplasmic reticulum (ER)-associated degradation of cystic fibrosis transmembrane conductance regulator is linked to retrograde translocation from the ER membrane. *J. Biol. Chem.* **274,** 2616–2624
38. Riordan, J. R. (2008) CFTR function and prospects for therapy. *Annu. Rev. Biochem.* **77,** 701–726
39. Younger, J. M., Chen, L., Ren, H. Y., Rosser, M. F., Turnbull, E. L., Fan, C. Y., Patterson, C., and Cyr, D. M. (2006) Sequential quality-control checkpoints triage misfolded cystic fibrosis transmembrane conductance regulator. *Cell* **126,** 571–582
40. Morito, D., Hirao, K., Oda, Y., Hosokawa, N., Tokunaga, F., Cyr, D. M., Tanaka, K., Iwai, K., and Nagata, K. (2008) Gp78 cooperates with RMA1 in endoplasmic reticulum-associated degradation of CFTRΔF508. *Mol. Biol. Cell* **19,** 1328–1336
41. Caohuy, H., Jozwik, C., and Pollard, H. B. (2009) Rescue of ΔF508-CFTR by the SGK1/Nedd4–2 signaling pathway. *J. Biol. Chem.* **284,** 25241–25253
42. Hatakeyama, S., Matsumoto, M., Yada, M., and Nakayama, K. I. (2004) Interaction of U-box-type ubiquitin-protein ligases (E3s) with molecular chaperones. *Genes Cells* **9,** 533–548
43. Oberdorf, J., and Skach, W. R. (2002) *In vitro* reconstitution of CFTR biogenesis and degradation. *Methods Mol. Med.* **70,** 295–310
44. Carlson, E., Bays, N., David, L., and Skach, W. R. (2005) Reticulocyte lysate as a model system to study endoplasmic reticulum membrane protein degradation. *Methods Mol. Biol.* **301,** 185–205
45. Matsumura, Y., and Skach, W. R. (2009) Protein export from endoplasmic reticulum to the cytosol: *In vitro* methods. in *Encyclopedia of Life Sciences* (Finazzi-Agrò, A., ed) John Wiley & Sons, Inc., New York, 10.1002/9780470015902.a0003430.pub2
46. Matsumura, Y., Rooney, L., and Skach, W. R. (2011) *In vitro* methods for CFTR biogenesis. *Methods Mol. Biol.* **741,** 233–253
47. Young, J. C., Hoogenraad, N. J., and Hartl, F. U. (2003) Molecular chaperones Hsp90 and Hsp70 deliver preproteins to the mitochondrial import receptor Tom70. *Cell* **112,** 41–50
48. Tzankov, S., Wong, M. J., Shi, K., Nassif, C., and Young, J. C. (2008) Functional divergence between co-chaperones of Hsc70. *J. Biol. Chem.* **283,** 27100–27109
49. Borges, J. C., Fischer, H., Craievich, A. F., and Ramos, C. H. (2005) Low resolution structural study of two human HSP40 chaperones in solution. DJA1 from subfamily A and DJB4 from subfamily B have different quaternary structures. *J. Biol. Chem.* **280,** 13671–13681
50. Carlson, E. J., Pitonzo, D., and Skach, W. R. (2006) p97 functions as an auxiliary factor to facilitate TM domain extraction during CFTR ER-associated degradation. *EMBO J.* **25,** 4557–4566
51. Brown, C. R., Martin, R. L., Hansen, W. J., Beckmann, R. P., and Welch, W. J. (1993) The constitutive and stress inducible forms of hsp 70 exhibit functional similarities and interact with one another in an ATP-dependent fashion. *J. Cell Biol.* **120,** 1101–1112
52. Matsumura, Y., Ban, N., Ueda, K., and Inagaki, N. (2006) Characterization and classification of ATP-binding cassette transporter ABCA3 mutants in fatal surfactant deficiency. *J. Biol. Chem.* **281,** 34503–34514
53. Strickland, E., Qu, B. H., Millen, L., and Thomas, P. J. (1997) The molecular chaperone Hsc70 assists the *in vitro* folding of the N-terminal nucleotide-binding domain of the cystic fibrosis transmembrane conductance regulator. *J. Biol. Chem.* **272,** 25421–25424
54. Oberdorf, J., Carlson, E. J., and Skach, W. R. (2006) Uncoupling proteasome peptidase and ATPase activities results in cytosolic release of an ER polytopic protein. *J. Cell Sci.* **119,** 303–313
55. Sondermann, H., Scheufler, C., Schneider, C., Hohfeld, J., Hartl, F. U., and Moarefi, I. (2001) Structure of a Bag/Hsc70 complex: convergent functional evolution of Hsp70 nucleotide exchange factors. *Science* **291,** 1553–1557
56. Scheufler, C., Brinker, A., Bourenkov, G., Pegoraro, S., Moroder, L., Bartunik, H., Hartl, F. U., and Moarefi, I. (2000) Structure of TPR domain-peptide complexes: critical elements in the assembly of the Hsp70-Hsp90 multichaperone machine. *Cell* **101,** 199–210
57. Graf, C., Stankiewicz, M., Nikolay, R., and Mayer, M. P. (2010) Insights into the conformational dynamics of the E3 ubiquitin ligase CHIP in complex with chaperones and E2 enzymes. *Biochemistry* **49,** 2121–2129
58. Ramsey, A. J., Russell, L. C., and Chinkers, M. (2009) C-terminal sequences of hsp70 and hsp90 as non-specific anchors for tetratricopeptide repeat (TPR) proteins. *Biochem. J.* **423,** 411–419
59. Muller, P., Ruckova, E., Halada, P., Coates, P. J., Hrstka, R., Lane, D. P., and Vojtesek, B. (2013) C-terminal phosphorylation of Hsp70 and Hsp90 regulates alternate binding to co-chaperones CHIP and HOP to determine cellular protein folding/degradation balances. *Oncogene* **32,** 3101–3110
60. Rubenstein, R. C., Egan, M. E, and Zeitlin, P. L. (1997) *In vitro* pharmacologic restoration of CFTR-mediated chloride transport with sodium 4-phenylbutyrate in cystic fibrosis epithelial cells containing ΔF508-CFTR. *J. Clin. Invest.* **100,** 2457–2465
61. Jiang, C., Fang, S. L., Xiao, Y. F., O'Connor, S. P., Nadler, S. G., Lee, D. W., Jefferson, D. M., Kaplan, J. M., Smith, A. E., and Cheng, S. H. (1998) Partial restoration of cAMP-stimulated CFTR chloride channel activity in ΔF508 cells by deoxyspergualin. *Am. J. Physiol.* **275,** C171-C178
62. Rubenstein, R. C., and Zeitlin, P. L. (1998) A pilot clinical trial of oral sodium 4-phenylbutyrate (Buphenyl) in ΔF508-homozygous cystic fibrosis patients: partial restoration of nasal epithelial CFTR function. *Am. J. Respir. Crit. Care Med.* **157,** 484–490
63. Park, H. J., Mylvaganum, M., McPherson, A., Fewell, S. W., Brodsky, J. L., and Lingwood, C. A. (2009) A soluble sulfogalactosyl ceramide mimic promotes ΔF508 CFTR escape from endoplasmic reticulum associated degradation. *Chem. Biol.* **16,** 461–470
64. Youker, R. T., Walsh, P., Beilharz, T., Lithgow, T., and Brodsky, J. L. (2004) Distinct roles for the Hsp40 and Hsp90 molecular chaperones during cystic fibrosis transmembrane conductance regulator degradation in yeast. *Mol. Biol. Cell* **15,** 4787–4797
65. Ahner, A., Nakatsukasa, K., Zhang, H., Frizzell, R. A., and Brodsky, J. L. (2007) Small heat-shock proteins select ΔF508-CFTR for endoplasmic reticulum-associated degradation. *Mol. Biol. Cell* **18,** 806–814
66. Frydman, J., and Höhfeld, J. (1997) Chaperones get in touch: the Hip-Hop connection. *Trends Biochem. Sci.* **22,** 87–92